

# Evaluation and application of argon and helium microstrip plasma for the determination of mercury by the cold vapor technique and optical emission spectrometry

Israel Jiménez Zapata · Pawel Pohl · Nicolas H. Bings · José A. C. Broekaert

Received: 8 January 2007 / Revised: 30 January 2007 / Accepted: 1 February 2007 / Published online: 24 February 2007  
© Springer-Verlag 2007

**Abstract** The suitability of a 2.45-GHz atmospheric pressure, low-power microwave microstrip plasma (MSP) operated with Ar and He for the determination of Hg by continuous-flow cold vapor (CV) generation, using SnCl<sub>2</sub>/HCl as the reducing agent, and optical emission spectrometry (OES) using a small CCD spectrometer was studied. The areas of stability for a discharge in the Ar and in the He MSP enclosed in a cylindrical channel in a quartz wafer were investigated. The excitation temperatures as measured for discharge gas atoms (Ar I, He I), and the electron number densities at 35–40 W and 15–400 mL min<sup>-1</sup> were found to be at the order of 3,200–5,500 K and  $0.8 \times 10^{14}$ – $1.6 \times 10^{14}$  cm<sup>-3</sup>, respectively. The relative intensity of the Hg I 253.6-nm line and the signal-to-background ratio as a function of the forward power (35–40 W) as well as of the flow rate of the working gas (15–400 mL min<sup>-1</sup>) were evaluated and discussed. For the selected measurement conditions, the Ar MSP was established to have the lower detection limit for Hg (0.6 ng mL<sup>-1</sup>) compared with the He MSP. The linearity range is up to 300 ng mL<sup>-1</sup> and the precision is on the order of 1–3%. With the optimized CV Ar MSP-OES method a determination of Hg in spiked domestic and natural waters at concentration levels of 20–100 µg L<sup>-1</sup> and an accuracy of 1–4% could be performed. In an NIST domestic sludge standard reference material, Hg (3.64 µg g<sup>-1</sup>) could be determined with a relative standard deviation of 4% and an agreement better than 4%.

**Keywords** Microwave microstrip plasma · Cold vapor generation · Mercury · Optical emission spectrometry

## Introduction

Despite the great progress in the instrumentation for atomic emission spectrometry due to innovations in the emission sources, the spectrometric systems and the detector technologies, there has been growing interest during the last decade in the miniaturization of the plasma discharge devices used for elemental spectrochemical analysis, including their use as chromatographic detectors [1–3]. Such activity aims at a reduction of different resources required for the operation of full-scale instruments. Indeed, it may lead to a substantial decrease of the overall costs of the measurements along with a much higher portability of the analytical spectrometric equipment [4, 5].

In the literature, the use of different electrodeless microdischarges and discharges operated with electrodes, comprising the microwave-induced microstrip plasma (MSP) [6, 7], the capacitively coupled microplasma [8], the direct current glow discharge microplasma [9], the stabilized capacitive plasma [10], and the microfabricated inductively coupled plasma [11], has been reported so far, mainly for the purpose of the determination of different analytes in the gaseous phase. They included different volatile hydrocarbons, their chlorinated derivatives, or other molecular gases such as SO<sub>2</sub>.

The application of the miniaturized plasma sources for the determination of the elements capable of forming vapors or volatile species through chemical vapor generation reactions performed in solution is much less frequent. So far, the analytical features of the microwave-induced plasma based on microstrip technology have been demon-

I. Jiménez Zapata · P. Pohl · N. H. Bings · J. A. C. Broekaert (✉)  
Institute for Inorganic and Applied Chemistry,  
Department of Chemistry, University of Hamburg,  
Martin-Luther-King-Platz 6,  
20146 Hamburg, Germany  
e-mail: jose.broekaert@chemie.uni-hamburg.de

strated by the determination of Hg in aqueous solutions through the cold vapor (CV) generation technique [7]. This situation can be attributed to the rather limited capabilities of the microplasma excitation sources to evaporate water vapor originating from the gas–liquid phase reaction/separation process or other reaction by-products accompanying the introduced volatile species of the analytes. Further, the low residence time of the sample in the plasma channel of the microdischarges as well as the relatively low excitation temperatures in these sources may have also a great influence [1].

Hence, investigations on the coupling of novel small-scale and chip-based analytical microplasma sources with different sample introduction techniques enabling an efficient loading of the plasma with the volatile species of the elements prior to their excitation and subsequent detection by atomic emission spectrometry or mass spectrometry are of special importance and significance for the development of miniaturized and portable measurement instrumentation.

In this work, the suitability and the applicability of 2.45-GHz miniaturized microwave Ar and He plasmas, based on microstrip technology, for the determination of Hg after an on-line continuous CV generation was studied in detail. For both Ar and He plasmas coupled with the CV technique, the effects of the forward power and the gas flow rate on the excitation temperature (Ar I, He I) and the electron number density were investigated. Further, their influence on the relative intensity of the Hg 253.6-nm line and the signal-to-background ratio (SBR) for that line was studied. Both MSPs were compared with reference to the limits of detection, the ranges of linearity, and the precision of the measurements. Furthermore, the analytical application of the CV Ar MSP will be shown to enable the determination of Hg in domestic and natural water samples as well as in a domestic sludge sample.

## Experimental

### Instrumentation

#### *Microstrip plasma source and spectrometer*

The atmospheric pressure, low-power microwave plasma based on the microstrip technology (MSP) was generated using a transistor-based 2.45-GHz microwave generator (Dirk Fischer Elektronik, Germany) with a maximal microwave power output of 40 W. The plasma was sustained fully inside the straight grown-in cylindrical channel (0.9-mm inner diameter) in a square sapphire wafer (30 mm long  $\times$  30 mm wide  $\times$  1.5 mm high) and was ignited with a spark as described previously [6, 12]. A 100-nm titanium adhesion layer covered both sides of the

sapphire plate. On one side of the wafer, a 2- $\mu$ m copper layer was sputtered and served as a ground electrode. The other side was provided with the microstrip lines (width of 0.8 mm) as it is schematically shown in Fig. 1a. The microwave power was introduced to the microstrip structure by a coaxial cable with a miniature connector and propagated along the inner side of the channel between the microstrip line and the ground electrode (Fig. 1b). The ground electrode was connected to a copper socket with an active air cooler (25 mm long  $\times$  25 mm wide). Ar and He were introduced into the analyte channel of the MSP structure by means of a 0.55-mm outer diameter polyethylene tube, after being loaded with the analyte, and served as discharge gases. For measuring and controlling the gas flow rates within the range from 15 to 400 mL min<sup>-1</sup>, a Bronkhorst HIGH-TEC (Netherlands) type F-201C-FB-33V mass flow meter was used.

For the acquisition of the spectra and the data recording, a miniaturized (89 mm long  $\times$  64 mm wide  $\times$  34 mm high) USB 2000 spectrometer (Ocean Optics, USA) with a built-in Sony ILX511 2048 element linear silicon CCD array detector coupled to a personal computer was employed. The optical bench design of the spectrometer was an asymmetric crossed Czerny–Turner system. The focal length of the spectrometer for input and output was 42 and 68 mm, respectively. A quartz optical fiber with a lens in front of it, placed 25 mm away from the emission source, was used to transmit the radiation to two fixed gratings in the CCD spectrometer. In addition, a quartz plate was used to protect the lens from hot gases released by the plasma.

### Cold vapor generation

The Hg CV generation and the separation of the analyte species from the reaction liquid were performed in a continuous-flow mode. The scheme of the CV system is given in Fig. 1c. A sample solution acidified with HCl and a reducing agent, i.e., a solution of SnCl<sub>2</sub> acidified with HCl, were pumped in parallel with a flow rate of 1 mL min<sup>-1</sup> to a T-piece, where the reagents were mixed. Then, the reaction mixture was carried on to a cylindrical gas–liquid separator (15-mm inner diameter, 100 mm long) for the separation of the Hg CV from the sample solution with the aid of the gas introduced at a flow rate of 15 mL min<sup>-1</sup>. The analyte CV and the accompanying solvent vapors were passed through a flask containing concentrated H<sub>2</sub>SO<sub>4</sub> for desolvation and were finally introduced into the MSP. Another approach for the water vapor removal made use of a Liebig condenser with the water jacket temperature at 274 K, or of a drying tube filled with Mg(ClO<sub>4</sub>)<sub>2</sub>·xH<sub>2</sub>O. The reaction liquid was removed from the separator by a peristaltic pump with a flow rate such that always 2 mL of solution was left inside the gas–liquid separator.

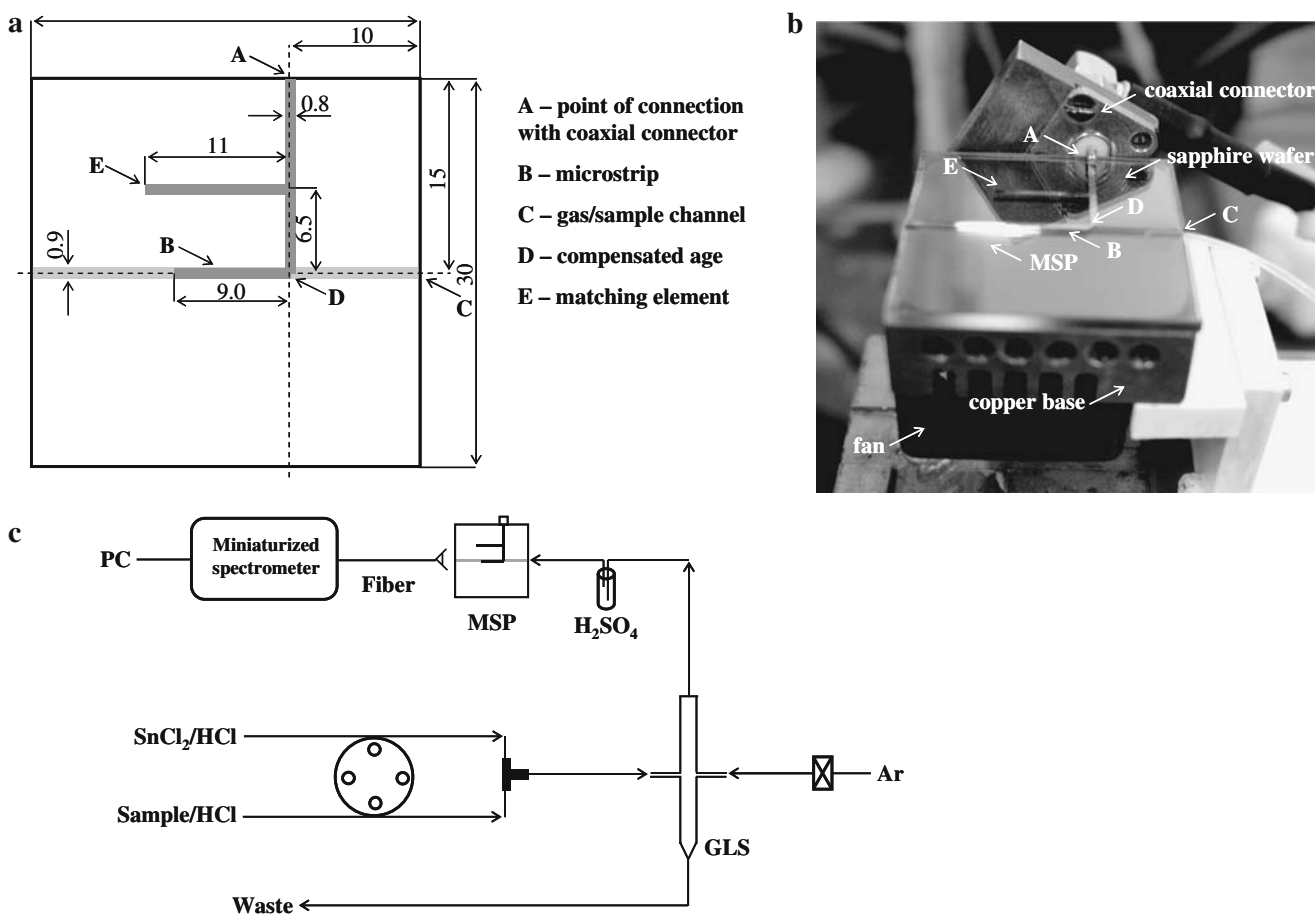


**Fig. 1** **a** Microstrip plasma (MSP) source using a sapphire wafer and microstrip lines. **b** Photograph of the Ar MSP coupled with the cold vapor (CV) technique. Gas flow rate  $15 \text{ mL min}^{-1}$ , forward power 40 W. **c** CV MSP optical emission spectrometry (OES) setup

### Reagents and standard solutions

All reagents used, namely, a  $10 \text{ g L}^{-1}$  standard solution of Hg (II), 32% (w/v) HCl, 65% (m/v)  $\text{HNO}_3$ , 96% (m/v)  $\text{H}_2\text{SO}_4$ ,  $\text{SnCl}_2 \cdot \text{H}_2\text{O}$ , NaCl, and  $\text{Mg}(\text{ClO}_4)_2 \cdot x\text{H}_2\text{O}$ , were of analytical grade and were purchased from Merck (Germany). Ar and He of 99.996% purity were supplied by Westfalen (Germany). Doubly distilled water was used throughout the work. Standard solutions of Hg with concentrations of 2.5, 5, 10, 20, 40, 100, 200, 300, and  $400 \text{ ng mL}^{-1}$  were prepared daily by dilution of the standard stock solution. The analyte solutions were acidified with HCl to a concentration of 2% (m/v). The solution of the reducing agent containing 5% (m/v) of  $\text{SnCl}_2$  in 2% (m/v) HCl was prepared by dissolving  $\text{SnCl}_2 \cdot \text{H}_2\text{O}$  in concentrated HCl and dilution with water as described in [13].

### Sample solutions

Synthetic sample solutions containing 50 and  $100 \text{ ng mL}^{-1}$  of Hg and NaCl at concentrations of 1, 2, 4, and 6% (m/v), respectively, were prepared by the dissolution of suitable

amounts of NaCl in water. The resulting solutions were spiked with the  $10 \text{ } \mu\text{g mL}^{-1}$  Hg solution to obtain the concentrations mentioned, acidified with concentrated HCl to a concentration of 2% (m/v), and finally diluted to 100 mL with water. In a corresponding way, 25  $\text{ng mL}^{-1}$  solutions of Hg with 50, 100, and  $250 \text{ ng mL}^{-1}$  of Ag, Al, B, Ba, Bi, Ca, Cd, Co, Cr, Cu, Fe, Ga, In, K, Li, Mg, Mn, Na, Ni, Pb, Sr, Tl, and Zn contained in the multielement Merck ICP standard IV solution were prepared. In the respective sample solutions, Hg was determined by CV Ar MSP optical emission spectrometry (OES) using synthetic standard solutions.

Samples of domestic and natural waters were collected in 0.5-L precleaned polyethylene bottles. After sampling, the solutions were acidified with concentrated HCl to a pH of 2 and spiked with  $10 \text{ } \mu\text{g mL}^{-1}$  Hg solution to obtain concentrations between 20 and  $100 \text{ ng mL}^{-1}$ . Prior to analysis, 50-mL portions of the spiked water samples were taken, acidified with concentrated HCl to a concentration of 2% (m/v), and diluted to 100 mL with water.

The domestic sludge standard reference material (NIST SRM 2781) was decomposed with the aid of a microwave-

assisted digestion oven according to the recommendations given in [14]. A portion of the material was initially oven-dried at 383 K for 2 h. Then, 0.25 g of the sample was weighed into the decomposition vessels, followed by the addition of 5 mL suprapure concentrated  $\text{HNO}_3$  and 5 mL suprapure concentrated  $\text{H}_2\text{SO}_4$ , and the mixture was subjected to the two-stage microwave oven digestion protocol. This included a first stage with a duration of 5 min as well as a power input of 300 W (35 bar, 313 K) and a second stage with a duration of 40 min as well as a power input of 300 W (35 bar, 463 K). After the digestion was complete, the nitrogen oxide fumes were removed by gently heating the vessels for about 20 min on a hot plate. After cooling, the contents of the vessels were quantitatively transferred to 50-mL calibrated flasks and the flasks were filled up with water. The determination of Hg in the respective samples of water and the digested reference material using CV Ar MSP-OES was performed with the use of three standard additions.

#### Excitation temperature and electron number density measurements

The excitation temperature ( $T_{\text{exc}}$ ) for Ar and He atoms (Ar I, He I) was determined assuming a Boltzmann distribution of the population of the excited atomic levels and using the least-squares method. The temperature was calculated from the slope of the  $\log(I\lambda/A)$  versus  $E$  (inverse centimeters) plot, while the uncertainty of the  $T_{\text{exc}}$  determination, at the most from 15 to 20%, was calculated from an estimation of the error of the slope. The selection of the atomic lines of Ar (seven lines, namely, 425.1, 425.9, 426.6, 427.2, 430.1, 433.4, and 434.5 nm) and He (five lines, namely, 402.6, 447.2, 471.3, 492.2, and 501.6 nm) for the Boltzmann plots was as described in the literature [15, 16]. The spectroscopic data for the Ar and He lines, i.e., the values of the upper-state energies and the transition probabilities, were taken from previously published compilations [17, 18].

The  $H_\beta$  486.1-nm line was used for the determination of the electron number density ( $n_e$ ). Its broadening was accepted to be mainly due to Stark broadening, and from this,  $n_e$  was calculated with the aid of the equation given by Griem [19]. The precision of  $n_e$  for three replicated measurements could be expected to be within 3–5%.

## Results and discussion

In order to evaluate the properties of the Ar and the He MSP for the excitation of Hg when its vapor is introduced into the discharge subsequent to the CV generation technique, the effect of the microwave forward power and

the Ar/He flow rate on  $T_{\text{exc}}$  as determined with Ar I and He I lines and  $n_e$  was investigated. In addition, the influence of these two experimental conditions on the background-corrected net Hg emission intensity and the SBR was studied as well. Therefore, the net analyte signals obtained under different conditions were measured, related to the highest value in the measurement series, and given as the relative intensities. The analytical line used was the atomic line of Hg I 253.6 nm [20]. Typical emission spectra of the Ar and the He MSPs coupled with the CV technique under optimized conditions are given in Fig. 2. Here it can be observed that the intensities of the Hg I 365.02-nm and Hg I 404.65-nm lines are much lower than that of the Hg I 253.65-nm line (0.036 and 0.02 versus 1.0 for the Ar MSP using CV generation with  $500 \text{ ng mL}^{-1}$  Hg in 2% HCl).

#### Area of plasma stability

The stability areas for the Ar and the He plasmas loaded with Hg vapor were determined in terms of the forward microwave power and the flow rates of the discharge gases. Both the Ar and the He plasmas, sustained inside the microstrip structure in the grown-in gas/analyte channel of 0.9-mm inner diameter, were found to be highly stable and reproducible. The Ar MSP was found to be stable at relatively low microwave power values compared with the plasma generated in the same structure with He as the discharge gas, especially in the range of low gas flow rates. Also the minimum power required to ignite the Ar MSP plasma was found to be up to 20% lower than the minimum power required to ignite the He MSP at the respective gas flow rates. Such a difference might be explained and attributed to the differences in the thermal conductivity and in the specific heat of both gases [21]. Furthermore, it also could be expected that as a result of the higher thermal conductivity of He, the He MSP would consume more

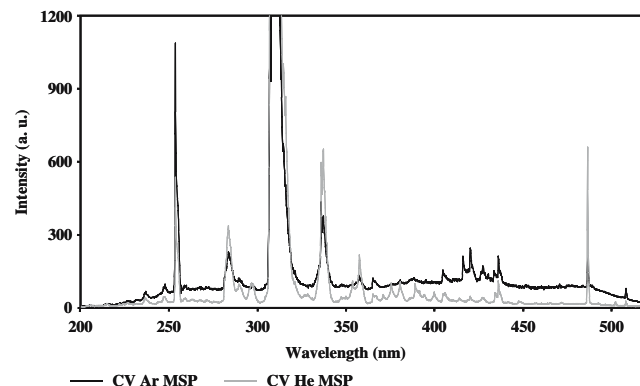


**Fig. 2** Emission spectra of Ar and He MSPs coupled with the CV technique. Concentration of Hg  $500 \text{ ng mL}^{-1}$ , gas flow rate  $15 \text{ mL min}^{-1}$ , forward power 40 W

energy than the respective Ar MSP and therefore would require a relatively high forward power compared with the Ar MSP. A similar effect was formerly observed with different microwave plasma structures coupled to chemical vapor generation techniques [20–22]. For drying the streams of Ar and He loaded with Hg vapors, a flask with concentrated H<sub>2</sub>SO<sub>4</sub> was used throughout the study. A water cooler was found to be less effective for that purpose in comparison with other setups of water vapor removal. The temperature of water jacket was set to 274 K since at higher temperatures the water vapor condensation was observed to be less efficient and resulted in instability of the plasma or in it being extinguished.

Also in the configuration of the discharges differences were observed. At a gas flow rate of 15 mL min<sup>-1</sup>, the Ar MSP was found to have the shape of a filament with a length between 3 and 9 mm depending on the forward power. For example, at a forward power of 40 W, the filament was found to extend about 5 mm out of the microstrip line, while the remaining part of the plasma filament (about 4 mm) was under the strip line. On increasing the gas flow rate to 110 mL min<sup>-1</sup>, a partial shift of the whole discharge into the gas channel was found to occur, and then, with a further increase of the argon flow rate, an increase of the plasma size occurred.

When using He as the working gas, a so-called suspended type of microplasma was observed, which was located near the end of the strip line, similar to what was described in [6]. At a gas flow rate of 15 mL min<sup>-1</sup>, the plasma length was found to be between 3 and 4 mm depending on the microwave power.

#### Influence of the forward power

With respect to the stability areas of the MSP, the effect of the microwave forward power on  $T_{\text{exc}}$ ,  $n_e$ , the relative intensities of Hg 253.6-nm line, and the SBRs was investigated in the range from 35 to 40 W and from 38.5 to 40 W for Ar and He, respectively. Both plasmas were operated at a gas flow rate of 15 mL min<sup>-1</sup> and continuously fed with Hg vapors using the CV system and a concentration of 40 ng mL<sup>-1</sup> Hg in the solutions.

#### Excitation temperature and electron number density

The dependence of  $T_{\text{exc}}$  and that of  $n_e$  on the power investigated are given in Fig. 3. Considering the measurement error,  $T_{\text{exc}}$  determined with Ar I lines was found to be constant (on average 5,500 K) in the range of power investigated. This indicates that for the Ar MSP most of the microwave power added contributed to the expansion of the plasma size rather than to an increase of  $T_{\text{exc}}$ . The power was not found to have any remarkable effect on the  $n_e$  of

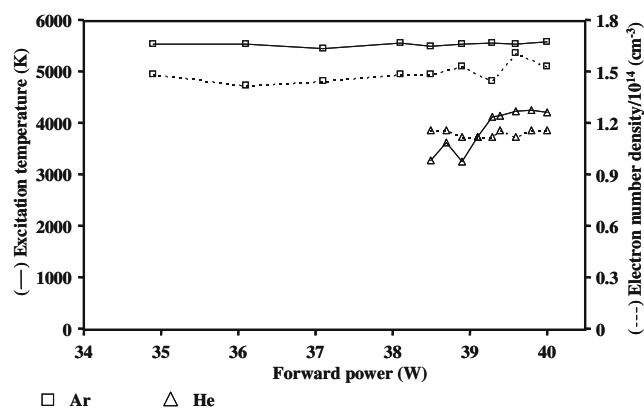


**Fig. 3** Dependence of excitation temperature ( $T_{\text{exc}}$ ) and electron number density ( $n_e$ ) on microwave forward power for Ar and He MSPs coupled with the CV technique. Concentration of Hg 40 ng mL<sup>-1</sup>, gas flow rate 15 mL min<sup>-1</sup>

the Ar MSP as the values of  $n_e$  measured were all within the range  $1.4 \times 10^{14}$ – $1.6 \times 10^{14}$  cm<sup>-3</sup>.

For the He MSP, a notable increase of the  $T_{\text{exc}}$  measured with the He I lines with the forward power could be observed. Indeed,  $T_{\text{exc}}$  was found to increase from 3,200 K for 38.5 W to 4,200 K for 40 W. Such behavior shows that a relatively high amount of the microwave power is consumed for the excitation of He atoms [21]. The  $n_e$  in the He MSP, however, was found to remain practically unaffected by the microwave forward power and its value was found to be  $1.1 \times 10^{14}$ – $1.2 \times 10^{14}$  cm<sup>-3</sup> in the whole range of the power investigated.

#### Analytical performance for the determination of Hg

For both MSPs investigated, an increase of the relative intensities of the Hg I 253.6-nm line with the forward power could be observed (Fig. 4). For the He MSP, this increase was found to be somewhat higher than that

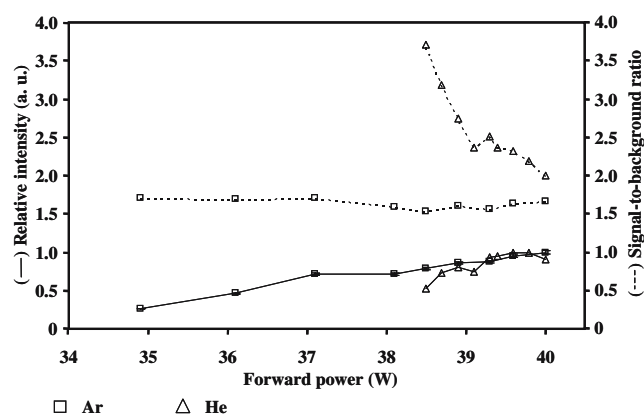


**Fig. 4** Effect of the forward power on the relative intensity of the Hg line and the signal-to background ratio (SBR) for Ar and He MSPs coupled with the CV technique. Concentration of Hg 40 ng mL<sup>-1</sup>, gas flow rate 15 mL min<sup>-1</sup>

found for the Ar MSP in the corresponding range of the power. The values of the SBR determined for the Ar MSP remained practically at about 1.6. This is in compliance with the behavior of  $T_{\text{exc}}$  determined with Ar I lines and with  $n_e$  for variation of the power. This might indicate that the electron excitation is likely to be balanced by the collisional excitation and recombination reactions [23]. As a result, an increase of the intensity of the Hg line with the forward power will be compensated by an increase of the background emission intensity, as was found to be the case.

For the He MSP, a deterioration of the SBR for the Hg I 253.6-nm line at increasing power was found. Referring to the rise of  $T_{\text{exc}}$  as determined with He I lines with increasing power and an almost unchanged level of  $n_e$  in the range of power examined, it was presumed that in this MSP, excitation by the electrons and collisions with excited He atoms and/or metastable He species formed in the discharge might play a role in the excitation of Hg. It was difficult to elucidate, however, which of the processes mentioned is more significant under the conditions investigated [15, 23–25]. In view of the relatively low forward power used in general for the MSP discharge in the present contribution, it could be expected that an increase of the power probably results in the collisional excitation dominating and an intensification of the recombination processes, leading to a greater increase of the background intensity than the analyte intensity.

#### Influence of the gas flow rate

The influence of the gas flow rate on  $T_{\text{exc}}$  as determined with Ar I and He I lines,  $n_e$ , as well as the relative intensities and the SBRs for the Hg I 253.6-nm line was investigated in the interval from 15 to 400 mL min<sup>-1</sup>. Both MSPs were operated at the maximal input power of 40 W. Hg was introduced with the continuous flow CV technique with solutions having a Hg concentration of 40 ng mL<sup>-1</sup>.

#### Excitation temperature and electron number density

Taking into consideration the error of the temperature measurements, it must be concluded that the flow rate of the working gas has practically no effect on  $T_{\text{exc}}$  in the Ar MSP. The average value of  $T_{\text{exc}}$  as measured with Ar I lines in the range of the gas flow rate investigated was close to 5,600 K (Fig. 5). The intensities of the atomic lines of Ar, e.g., at 415.5, 419.8, and 433.5 nm, dropped, however, up to 160 mL min<sup>-1</sup> (about 8% on average compared with the intensities obtained at a flow rate of 15 mL min<sup>-1</sup>) and then were found to steadily increase with the gas flow rate up to 400 mL min<sup>-1</sup> (about 15–30% compared with the intensities obtained at a flow rate of 15 mL min<sup>-1</sup>). No specific

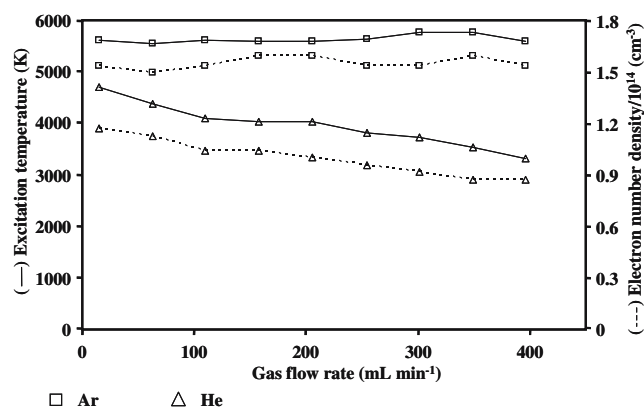


**Fig. 5** Dependence of  $T_{\text{exc}}$  and  $n_e$  on the gas flow rate for Ar and He MSPs coupled with the CV technique. Concentration of Hg 40 ng mL<sup>-1</sup>, forward power 40 W

trend for variations of  $n_e$  for the Ar MSP with the gas flow rate could be observed. The values of  $n_e$  were found to oscillate around a mean value of  $1.5 \times 10^{14}$  cm<sup>-3</sup>.

For the He MSP, an increase of the gas flow rate was found to result in a significant decrease of  $T_{\text{exc}}$  as measured with He I lines and of  $n_e$ . Indeed, changes from 4,700 K and  $1.2 \times 10^{14}$  cm<sup>-3</sup> for a He flow rate of 15 mL min<sup>-1</sup> to 3,300 K and  $0.8 \times 10^{14}$  cm<sup>-3</sup> for a He flow rate of 400 mL min<sup>-1</sup> could be observed. This behavior, being in agreement with previous findings reported for other microwave He plasmas [20, 25, 26], presumably resulted from a deactivation of the excited He atoms by collisions with He ground-state atoms. The profiles of the changes of  $T_{\text{exc}}$  and  $n_e$  determined for the He MSP were found to correspond to those of the intensity of the atomic spectra of He. For example, for the most intense He I lines at 388.9, 447.1, and 501.6 nm, respectively, one could notice a small increase in the emission intensities up to a flow rate of 110 mL min<sup>-1</sup> and then a gradual decrease with increasing gas flow rate.

#### Analytical performance for the determination of Hg

For both MSPs studied, a decrease of the relative intensities and the SBRs with the gas flow rate was found to occur (Fig. 6). Considering the dependence of  $T_{\text{exc}}$  as measured with Ar I lines and of  $n_e$  on the gas flow rate for the Ar MSP, it was suspected that the decrease of the intensity of the Hg line by about 40% on the whole was associated with the short residence time of the analyte in the plasma.

The decrease of the Hg line intensity with the gas flow rate for the He MSP was found to be considerably higher, namely, 60% on average, than that observed for the Ar MSP. It could be that apart from the decrease of the residence time of the analyte in the small-volume He MSP the “cooling” of the plasma by the deexcitation process has an additional effect on the excitation of Hg and, in

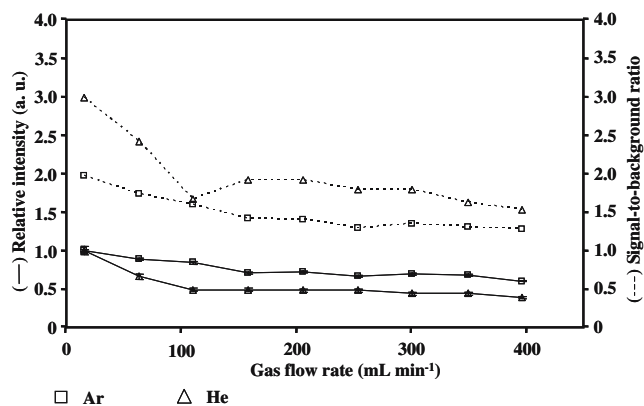


**Fig. 6** Effect of the gas flow rate on the relative intensity of the Hg line and its SBR for Ar and He MSPs coupled with the CV technique. Concentration of Hg 40 ng mL<sup>-1</sup>, forward power 40 W

consequence, the analytical response for that element. The results for the SBRs corresponded well with those for the relative intensities of the Hg line, the values of which also decreased with an increase of the gas flow rate for both MSPs.

#### Effect of different setups for water vapor removal

The generation of CV of Hg is accompanied by the formation of water vapor which has been recognized to influence the stability and the excitation properties of the microwave plasmas. Normally, the use of a desolvation trap is required to remove the residual water vapor before allowing the analyte vapor cloud to enter into the excitation sources [22, 26].

In the present study, different desolvation setups for drying the analyte vapors after the gas–liquid phase separation before their entry into the Ar and He MSPs were examined and compared (Fig. 7). It was found that the setup with the Mg(ClO<sub>4</sub>)<sub>2</sub>-filled tube and the flask with concentrated H<sub>2</sub>SO<sub>4</sub> with and without the cooler produced the highest relative intensities of the Hg line for both MSPs. Corresponding results for both plasmas were also achieved using a flask with concentrated H<sub>2</sub>SO<sub>4</sub> only. The application of the water-vapor cooler only was found to be less effective. A disadvantage of the setups with the drying tube, however, was the relatively fast exhaustion of the absorption capacity of Mg(ClO<sub>4</sub>)<sub>2</sub> for H<sub>2</sub>O, which then led to absorption of the analyte and deterioration of the detection limit for Hg. Therefore, the use of a flask containing concentrated H<sub>2</sub>SO<sub>4</sub> was chosen for the desolvation of the analyte vapor because it was easy to install and it can be used for a relatively long time as well.

#### Analytical performance and application

Under the optimum conditions, namely, a gas flow rate of 15 mL min<sup>-1</sup> and a forward power of 40 W, the sensitivity,

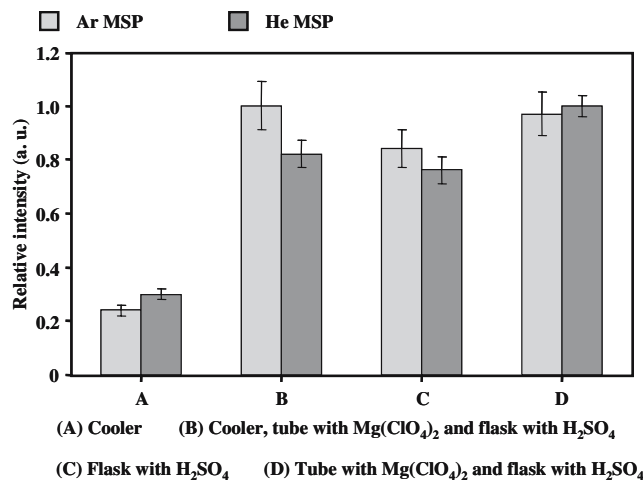


**Fig. 7** Effect of different setups for the removal of water vapor on the analytical signal for Hg in CV MSP-OES. Concentration of Hg 40 ng mL<sup>-1</sup>, gas flow rate 15 mL min<sup>-1</sup>, forward power 40 W

the detection limit, and the measurement precision at different concentrations of Hg were assessed as analytical figures of merit for the Ar and He MSPs coupled with the CV generation technique. A linear calibration curve for the determination of Hg by the CV Ar MSP-OES (Fig. 8) was obtained for standard solutions at concentrations between 2.5 and 300 ng mL<sup>-1</sup> with a correlation coefficient of 0.9988. The detection limit based on the 3 $\sigma_{\text{blank}}$  criterion was found to be 0.64 ng mL<sup>-1</sup> and is comparable to that reported lately for the CV microwave-induced plasma OES system with a microwave plasma torch [20]. It is somewhat higher than the value of 0.05 ng mL<sup>-1</sup> reported by Engel et al. [7], which may be due to the poorer resolution of the spectrometer used for our measurements. The measurement precision, expressed by the relative standard deviation

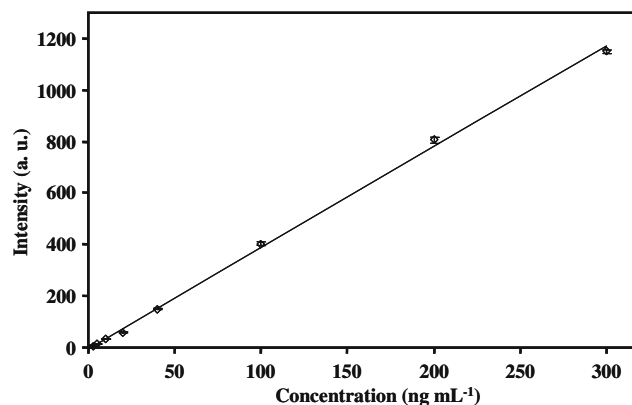


**Fig. 8** Calibration curve for the determination of Hg by CV Ar MSP-OES. Concentrations of Hg standard solutions between 2.5 and 300 ng mL<sup>-1</sup>, Ar flow rate 15 mL min<sup>-1</sup>, forward power 40 W

(RSD) for  $n=3$ , for low concentrations of Hg, i.e., from 5 to 20 ng mL<sup>-1</sup>, varied from 9 to 3%. For higher analyte concentrations, i.e., from 40 to 300 ng mL<sup>-1</sup>, the RSD values were from 2 to 0.7%. Despite the higher microwave power required for the analyte excitation in the He MSP, this plasma showed a poorer analytical performance for the determination of Hg. A shorter dynamic range (up to 100 ng mL<sup>-1</sup>) as well as a poorer limit of detection (1.1 ng mL<sup>-1</sup>) were obtained. For that reason, the Ar MSP was applied for the determination of Hg in the samples.

A series of artificial water samples containing Hg and different amounts of NaCl were analyzed using a calibration with pure aqueous solutions containing Hg only to establish the influence of major seawater, saline and wastewater concomitants on the determination of Hg, similar to what was reported in [13]. In addition, the solutions containing the multielement matrix were also analyzed (Table 1). None of the foreign ions present in those samples was found to reach the plasma; therefore, the interferences were presumed to occur during the Hg CV generation and separation process. In the case of a high Hg concentration, it could be observed that the presence of NaCl at a concentration of 1, 2, 4, and 6% (m/v), respectively, could be tolerated as the recoveries for Hg achieved were within 92–104%. For lower Hg concentrations, the recoveries in the presence of a high content of NaCl in the solution were found to decrease. Also the presence of the elements in the multielement solution at a concentration higher than 5 µg mL<sup>-1</sup> was observed to have a negative effect on the determination of Hg.

**Table 1** Determination of Hg in artificial water samples by means of cold vapor Ar microstrip plasma optical emission spectrometry using calibration with aqueous solutions containing Hg only

Sample	Added (ng mL <sup>-1</sup> )	Found (ng mL <sup>-1</sup> )	Recovery (%)
Water containing NaCl matrix			
1% (m/v)	100	91.6±2.2	91.6±2.2
2% (m/v)	100	94.7±1.5	94.7±1.5
4% (m/v)	100	106±4	106±4
6% (m/v)	100	94.7±1.8	94.7±1.8
1% (m/v)	50.0	54.6±4.5	109±9
2% (m/v)	50.0	47.2±4.3	94.3±8.5
4% (m/v)	50.0	40.0±3.1	80.0±6.2
6% (m/v)	50.0	31.2±3.1	62.3±6.3
Water containing multielement matrix <sup>a</sup>			
50 ng mL <sup>-1</sup>	25.0	25.0±1.8	100±1
100 ng mL <sup>-1</sup>	25.0	22.7±0.8	90.8±3.4
250 ng mL <sup>-1</sup>	25.0	19.2±2.2	76.9±8.9

Results are mean values ( $n=3$ ) ± the standard deviations

<sup>a</sup> Multielement ICP standard IV containing Ag, Al, B, Ba, Bi, Ca, Cd, Co, Cr, Cu, Fe, Ga, In, K, Li, Mg, Mn, Na, Ni, Pb, Sr, Tl, and Zn was added.

The analysis of real samples was carried out for different types of samples (Table 2). Owing to absence of Hg in the samples of domestic and natural waters, they were spiked with different concentrations of Hg. The standard reference material of a domestic sludge was decomposed in the mixture of concentrated HNO<sub>3</sub> and H<sub>2</sub>SO<sub>4</sub> using microwave-assisted digestion and Hg was determined in the samples by CV Ar MSP-OES using three standard additions. Very good recoveries were obtained, proving the reliability and the accuracy of the method developed.

## Conclusions

In the present study, it could be demonstrated that the Ar and He MSPs operated in a sapphire chip in the case of a miniaturized CCD array spectrometer are suitable for the determination of Hg with the aid of the CV technique. The MSP sustained with Ar as the working gas was found to have a better analytical performance than the He plasma at a microwave power input below 40 W. This is reflected in the detection limit for Hg, the stability, and the tolerance to analyte loading. In comparison with previously published works considering the MSP [6, 12], the experimental setup for CV MSP-OES through the use of the spectrometer shows further miniaturization of the measurement system while maintaining the possibility of its application in the analysis of environmental samples. In view of a growing development of battery-powered oscillators and a new generation of miniature high-resolution spectrometers, the Ar MSP coupled with CV presented may be an integrated part of measurement devices fulfilling the requirements of the micro-total analysis systems.

The analyses of real samples and the certified reference material confirm the possibilities of the MSP technology for elemental Hg determinations as well as for its further

**Table 2** Determination of Hg in spiked water samples and in a certified reference material by means of cold vapor Ar microstrip plasma optical emission spectrometry using three standard additions

Sample	Added (ng mL <sup>-1</sup> )	Found (ng mL <sup>-1</sup> )	Recovery (%)
Domestic water 1	100	101±1	101±1
Domestic water 2	30.0	30.3±3.0	101±10
Natural water <sup>a</sup> 1	50.0	48.3±2.0	96.6±4.0
Natural water <sup>a</sup> 2	20.0	19.1±1.0	95.5±5.0
Domestic sludge <sup>b</sup>	3.64±0.25 <sup>c</sup>	3.80±0.15 <sup>d</sup>	104±4

Results are mean values ( $n=3$ ) ± the standard deviations

<sup>a</sup> Lake Alster (Hamburg, Germany)

<sup>b</sup> NIST standard reference material SRM 2781

<sup>c</sup> Certified value (µg g<sup>-1</sup>)

<sup>d</sup> In units of micrograms per gram



application and for the determination of other volatile species using chemical and electrochemical hydride generation.

**Acknowledgements** I.J.Z. expresses his gratitude to the German Academic Exchange Service (DAAD) for granting a PhD scholarship. P.P. acknowledges the Alexander von Humboldt Foundation for the grant of a research fellowship.

## References

1. Broekaert JAC, Siemens V (2004) *Anal Bioanal Chem* 380:185–189
2. Karanassios V (2004) *Spectrochim Acta Part B* 59:909–928
3. Miclea M, Kunze K, Franzke J, Niemax K (2002) *Spectrochim Acta Part B* 57:1585–1592
4. Franzke J, Kunze K, Miclea M, Niemax K (2003) *J Anal At Spectrom* 18:802–807
5. Broekaert JAC (2002) *Anal Bioanal Chem* 374:182–187
6. Bilgic AM, Voges E, Engel U, Broekaert JAC (2000) *J Anal At Spectrom* 15:579–580
7. Engel U, Bilgic AM, Haase O, Voges E, Broekaert JAC (2000) *Anal Chem* 72:193–197
8. Bass A, Chevalier C, Blades MW (2001) *J Anal At Spectrom* 16:919–921
9. Eijkel JCT, Stoeri H, Manz A (2000) *Anal Chem* 72:2547–2552
10. Quan X, Chen S, Platzer B, Chen J, Gfrerer M (2002) *Spectrochim Acta Part B* 57:189–199
11. Minayeva OB, Hopwood JA (2003) *J Anal At Spectrom* 18:856–863
12. Schermer S, Bings NH, Bilgic AM, Stonies R, Voges E, Broekaert JAC (2003) *Spectrochim Acta Part B* 58:1585–1596
13. Haase O, Klare M, Kregel-Rothensee K, Broekaert JAC (1998) *Analyst* 123:1219–1222
14. Saraswati R, Vetter TW, Watters RL (1995) *Analyst* 120:95–99
15. Tanabe K, Haraguchi H, Fuwa K (1983) *Spectrochim Acta Part B* 38:49–60
16. Cotrino J, Saez M, Quintero MC, Menendez A, Sanchez Uria JE, Sanz Medel A (1992) *Spectrochim Acta Part B* 47:425–435
17. Wiese WL, Martin GA (1980) Wavelengths and transition probabilities of atoms and atomic ions. US Department of Commerce, National Bureau of Standards, Washington
18. Wiese WL, Smith MW, Miles BM (1969) Wavelengths and atomic transition probabilities for atoms and atomic ions. US Government Printing Office, Washington
19. Griem HR (1974) *Spectral line broadening by plasmas*. Academic, New York
20. Camuna Aguilar JF, Pereiro Garcia R, Sanchez Uria JE, Sanz Medel A (1994) *Spectrochim Acta Part B* 49:457–484
21. Abdillahi MM, Snook RD (1986) *Analyst* 111:265–267
22. Bulska E, Broekaert JAC, Tschoepel P, Toelg G (1993) *Anal Chim Acta* 276:377–384
23. Huang M (1996) *Microchem J* 53:79–87
24. Brandl PG, Carnahan JW (1994) *Spectrochim Acta Part B* 49:105–115
25. Houpt PM (1976) *Anal Chim Acta* 86:129–138
26. Costa Fernandez JM, Pereiro Garcia R, Sanz Medel A, Bordel Garcia N (1995) *J Anal At Spectrom* 10:649–654